2018

Condensation and evaporation local heat transfer characteristics of the refrigerant mixture of R1123 and R32 inside a plate heat exchanger

Keishi Kariya
Saga university, Saga, Japan, kariya@me.saga-u.ac.jp

Koki Sonoda
Saga univarsity, Japan, 16575010@edu.cc.saga-u.ac.jp

Syota Wakasugi
Saga univarsity, Japan, 17575030@edu.cc.saga-u.ac.jp

Yamato Eshima
miyara@me.saga-u.ac.jp

Condensation and evaporation local heat transfer characteristics of the refrigerant mixture of R1123 and R32 inside a plate heat exchanger

Keishi KARIYA[1]*, Koki SONODA[2] and Akio MIYARA[1]

[1] Department of Mechanical Engineering, Saga University, 1 Honjo-machi, Saga, 840-8502, Japan
Tel: +81-952-28-8608, E-mail: kariya@me.saga-u.ac.jp

[2] Graduate School of Science and Engineering, Saga University, 1 Honjo-machi, Saga, 840-8502, Japan

ABSTRACT

In the present study, condensation and evaporation local heat transfer coefficients of the refrigerant mixture of R1123 and R32 inside a brazed plate heat exchanger were investigated by using a test section which is combined with two grooved stainless steel plates. In the test section, wall temperature distribution was measured. The test section consists of eight plates; two of them were processed herringbone for refrigerant flow channel other two flat plates are set for cooling plate for refrigerant, and another consist on cooling water flow channel. In order to measure local heat transfer and temperature distribution, five thermocouples were set on flow direction for each wall temperature measurement of the refrigerant side and heat source water side. Local heat transfer coefficient were calculated from local wall temperature of refrigerant side, saturation temperature and local heat flux obtained by temperature gradient between heat transfer surface of refrigerant side and heat source side.

1. INTRODUCTION

In the technical field of refrigeration and air-conditioning, plate heat exchangers are getting attention due to their compactness and high thermal efficiency. Although these were mainly designed for liquid single-phase heat exchanger, its application was extended to two phase heat exchangers such as condensers and evaporators. Condensation and evaporation heat transfer coefficients in plate heat exchangers have been studied by many researchers. Most of the existing literatures, however, discussed mainly overall heat transfer characteristics (Longo et al., 2010, Yan et al., 1999). Local heat transfer behavior has not been clarified sufficiently. Because of the effects on global warming by the refrigerants used in the present heat pump/refrigeration systems, new synthetic refrigerants, hydrofluoroolefins (HFOs), which have low global warming potential (GWP) are recently getting attention as next generation refrigerants (Miyara et al., 2012, Kariya et al., 2016, Zhang et al., 2017). However, many of HFOs has low flammability and expensive. Therefore, systems in which small amount of refrigerant is charged are required. When the plate heat exchangers are used as evaporator and/or condenser, maldistribution of refrigerant flow occurs in channels between the plates and headers to distribute it to the channels. This maldistribution deteriorates the heat exchanger performance. And local heat transfer coefficient may vary at flow direction and width direction in plate heat exchangers. It is important to investigate flow characteristics for understanding the heat transfer characteristic and for enhancing the heat transfer. Only a few reports about experimental flow observation of two phase flow in the plate heat exchanger. Asano et al. (2007) carried out the visualization of gas-liquid two phase flow by neutron radiography. Void fraction distributions in the plate heat exchanger were also measured. Arima et al. (2012) carried out flow observations and void fraction measurements on evaporation of ammonia flowing in parallel plates instead of an actual channel of plate heat exchangers. Experiments on condensation and evaporation heat transfer of low GWP refrigerants, R1234yf and R1234ze(E), in a plate heat exchanger have been carried out by Longo et al. (2012, 2013, 2014). Heat transfer coefficients and pressure drops in the condensation and evaporation of R1234ze(E) and R1234yf were measured and effects of saturation temperature, refrigerant mass flux and vapour super-heating are discussed. The data have been obtained from overall heat transfer performance and there is no sufficient discussion about local heat transfer characteristics. The local heat transfer coefficient varies not only flow direction but also width direction by gas-liquid distribution. In order to further understand the heat transfer characteristics, information about the local heat transfer is necessary. But measurements of local wall temperatures and heat fluxes are difficult because of the complicated structure. In the present study, a specially designed test section has been constructed for the measurement of local heat transfer

coefficient. Experiments on condensation and evaporation heat transfer of a low GWP refrigerant, binary mixture R1123/R32 40:60 mass% were carried out and local heat transfer characteristics were discussed.

2. EXPERIMENTAL APPARATUS AND THE DATA REDUCTION METHOD

2.1 Flow Loop of Refrigerant

Figure 1 shows experimental flow loop of refrigerant. It mainly consists of magnet pump, pre-heater, test section and after condenser. After the refrigerant flows from magnet pump, mass flow rate is measured by coriolis flow meter. Then the refrigerant is heated by the pre-heater to set a designated enthalpy condition at the inlet of test section. After the refrigerant flows out through the test section, it is cooled by the after condenser to keep a certain subcooling. And the subcooled liquid comes back to the magnet pump. Mixing chambers are installed at inlet of the pre-heater and inlet and outlet of the test section to obtain the bulk enthalpy from measured refrigerant pressure and temperature at the mixing chamber. The refrigerant is heated or cooled by water of which temperature is controlled by thermostatic bath. The flow rate of refrigerant is controlled by the flow control valve and the rotation speed of magnet pump.

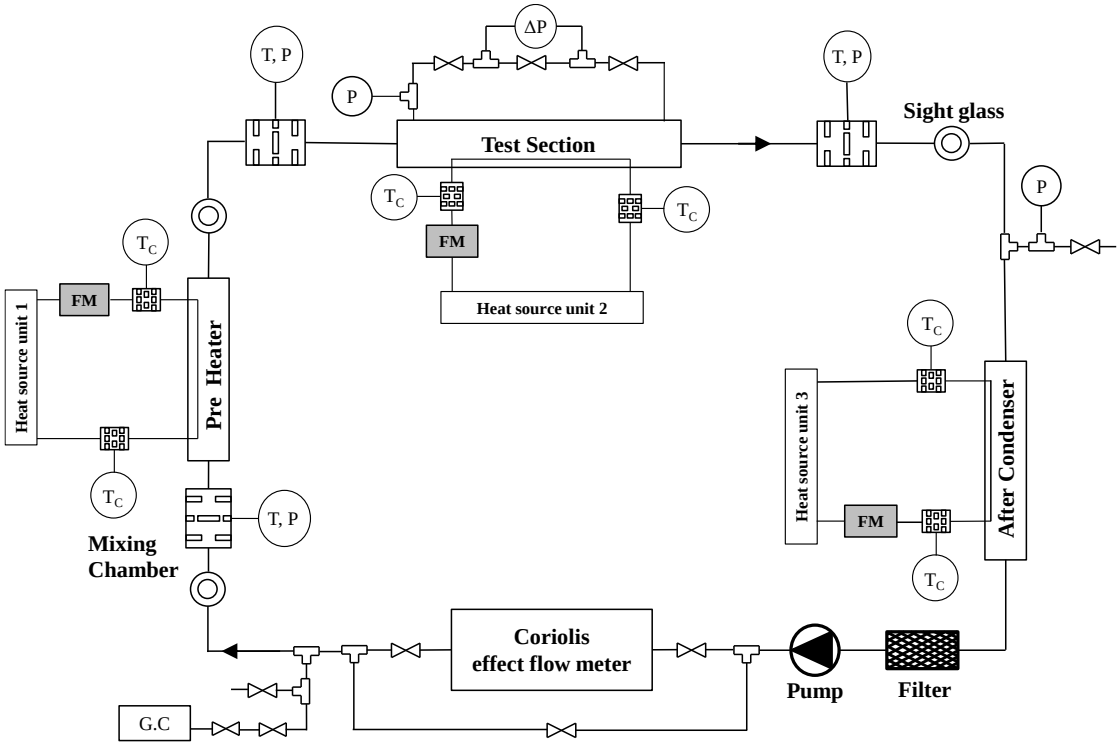

Figure 1: Schematic diagram of refrigerant flow loop

2.2 Test Section

For the measurement of local heat transfer characteristics of plate heat exchanger, a specially designed test section has been produced same as our previous study Kariya et al., 2016). Figure 2 shows the schematic of test section and the installed points of thermocouples with the photograph. Chevron shape grooved are dug over a stainless steel plate of which length, width and thickness are 186mm, 84mm and 5mm, respectively. The pitch and depth are 5.6mm and 1.5mm, respectively. A channel of the plate heat exchanger where the refrigerant flows is constructed by facing two grooved plats. Next of the grooved plates, flat plates are set to measure heat flux. Plates for the water channel are set outside of the flat plates. Whole of the test section is constructed with eight different kinds of plates which are brazed each other. The chevron directions of each plates which make a refrigerant flow channel are reversely assembled so that heat transfer enhance. The flat plates with 10mm in thickness have holes of 1.6mm in diameter on both sides where wire T-type thermocouples are installed and temperatures are measured. Positions of the temperature measurement are set at 4, 12, 20, 28, 36, 44, 52, 60 and 64 mm from end face of the cross section of

the channel. Position of the inlet and outlet of refrigerant are 20 mm. Temperatures of local heat transfer surface at refrigerant and water sides are estimated from the measured temperature as explained later. The temperatures are also used to calculate the heat flux and heat transfer coefficient. The water channels consist of flat plates and the channel height is 5mm. Water flows into the channels from both sides of the test section, front and back. It should be noted, surface which have the inlet/outlet ports of refrigerant is called as inlet side and another side is call as opposite side. In addition, the center region is set for temperature measurement between the inlet and the opposite side as shown in the figure. The geometrical characteristics of the test section are listed in Table 1.

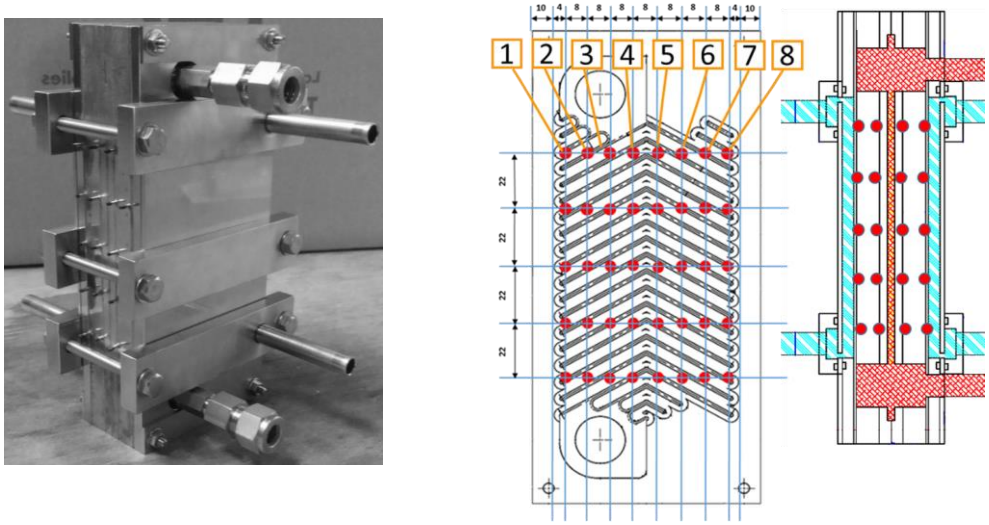

Figure 2: Photograph and Schematic of test section and place of temperature measurement

Table 1: Geometrical characteristics of the test section

Fluid flow plate length (mm)	117.5
Plate width (mm)	64
Area of the plate (m^2)	0.75
Corrugation type	Chevron
Angle of the corrugation (°)	60
Corrugation pitch (mm)	5.6
Number of plates	8
Number of channels on refrigerant side	1
Number of channels on water side	2

2.3 Data Reduction Method

By assuming the steady sate one-dimensional heat conduction, the local heat flux q_x in test section is calculated from the temperatures measured at both sides of 10mm thick flat plates.

$$q_x = \frac{T_{w,ref} - T_{w,water}}{l_1} \lambda \tag{1}$$

Where $T_{w,ref,}$ is temperature of measurement place of refrigerant side, $T_{w,\,water}$ is temperature of measurement place of water side, l_1 is distance between each K-type thermocouples. λ is the thermal conductivity of the stainless steel plate. Wall surface temperature of refrigerant side is calculated with the following equation where the linear temperature distribution is assumed and the temperature is extrapolated to the representative of surface of refrigerant

side. l_2 in the equation is the distance between the K-type thermocouple and the average surface of the refrigerant side.

$$T_{wall,x} = T_{w.ref} \pm \frac{q_x l_2}{\lambda} \tag{2}$$

The plus-minus sign means the plus for condensation experiment, and the minus for evaporation experiment.
The local heat transfer coefficient h_x is defined with the following equation.

$$h_x = \frac{q_x}{T_{wall,x} - T_{sat}} \tag{3}$$

Where, T_{sat} is the saturation temperature of refrigerant which is calculated from measured pressure. q_x and $T_{wall,x}$ are calculated with Eq.(1) and (2), respectively.
The local thermodynamic equivalent quality x and saturation temperature (boiling point) T_{sat} in the plate channel are calculated from mass balance of low-boiling point component Eq. (5) and correlation of saturation temperature obtained by thermodynamic properties measurement (Higashi and Akasaka, 2016) as below;

$$x = \frac{m_V}{m} \tag{4}$$

$$w_L = \frac{w_b}{1 + x\left(\frac{w_V}{w_L} - 1\right)} \tag{5}$$

$$T_{sat} = f(w_L, P) \tag{6}$$

Where w_{L}, w_{V}, w_{b} indicate liquid, vapour and bulk mass concentration, respectively.
Finally, the local specific enthalpy in the test section is calculated from mass flow rate $\dot{m}$ and the heat transfer rate from the inlet to a certain point which is obtained by integrating the heat flux, as expressed with the following equation.

$$i_x = i_{in} + \frac{1}{\dot{m}} \int_0^{A_x} q dA \tag{7}$$

3. RESULT AND DISCUSSION

3.1 Experimental Condition

Table 2 indicates experimental conditions of the present study. Refrigerant tested is R1123/R32 40/60 mass % binary mixture which is one of the promising candidates of the next generation refrigerants and has the low GWP. Pure R32 measurement was also conducted for comparison with the binary mixture. Flow direction of the refrigerant is the downward for condensation test and the upward for evaporation test. Saturated temperature are 20 °C and 10 °C for condensation and evaporation tests, respectively. Mass flux conditions are 10 and 20 kg/(m^2·s) in both experiments. In the case of mass flux 10 kg/(m^2·s) conditions for both condensation and evaporation experiment, temperature of cooling water (heat source at the test section) is controlled in order that the refrigerant flows into the test section as nearly saturated vapor (condensation) or liquid (evaporation) state and flows out as nearly saturated liquid (condensation) or vapor (evaporation). In the condition of mass flux 20 kg/(m^2·s), both condensation and evaporation experiment are carried out in two inlet conditions in order to measure large quality region. In the condensation and evaporation experiment, inlet conditions are nearly saturated vapor (condensation) or saturated liquid (condensation) and x = 0.5 (condensation and evaporation) with the same heat flux condition of mass flux 10 kg/(m^2·s).

Table 2: Experimental conditions

	Refrigerant	Flow direction	T_{sat} [°C]	G [kg/(m^2·s)]
Condensation	Pure R32 R1123/R32 40/60 mass% mixture	Downward	20	10 and 20
Evaporation	Pure R32 R1123/R32 40/60 mass% mixture	Upward	10	10 and 20

3.2 Results of Condensation

Figure 3, 4 and 5 show local heat transfer coefficient distribution in the case of the binary mixture of the condensation experiment at x = 0.93, 0.57 and 0.17 with mass flux G = 10 [kg/m^{2}s], respectively. The value of local condensation heat transfer coefficient of vertical plate calculated by the Nusselt's liquid-film theory shown in Eq. (8) is also shown these figures by solid line.

$$h_{x,Nusselt} = 0.707\left[\frac{\lambda_L^3 g \rho_L^2 L}{\mu_L l_3 (T_{sat} - T_{wall,x})}\right]^{0.25} \tag{8}$$

Where g is gravitational acceleration, ρ_L is liquid density, L is latent heat, μ_L is liquid viscosity, l_3 is length of heat transfer surface, $T_{wall,x}$ is average of wall temperature in horizontal direction.

As shown in the figures, the position indicating maximum value of heat transfer coefficient is about 20 mm due to the inlet refrigerant effect and heat transfer coefficient represent the minimum value at the end face of the channel. It is also found that measurements are higher than calculation by Eq. (8) except for the value at the end face. The similar tendency is obtained in our previous study (Kawazoe et. al, 2015, Kariya et. al, 2016). From this result, it is inferred that maldistribution of condensate flow occurs in the channel of plate heat exchangers.

Figure 6 shows the average heat transfer coefficient of cross section versus quality at the same condition in Figure 3 to 5. The values of quality are average values of horizontal cross section which are calculated from heat balance of the measured heat flux as explained in previous section. As quality decreases, heat transfer coefficient slightly decreases as a general behaviour of condensation. The thickness of liquid film increases with increase of wetness and it generally prevents heat transfer. In our observation of air-water two phase flow (Eshima et al., 2013), liquid flow mainly in the center and both edge of the plate. This tendency can be seen slightly from the present experimental value at the near inlet and center position of the channel.

Figure 7 and 8 show local heat transfer coefficient distribution in the case of the pure R32 of the condensation experiment at x = 0.92 and 0.57 with mass flux G = 10 [kg/m^{2}s], respectively. Compared value of heat transfer coefficient in Figure 7 with that in Figure 3, both values are similar independent on the kind of refrigerants. Same tendency can be seen between Figure 4 and 8. In general, condensation heat transfer coefficient is effected by liquid thermal conductivity of the liquid phase. In this case, liquid thermal conductivity of the binary mixture is lower than pure R32. Therefore, the heat transfer coefficient of the binary mixture seemed to be lower. After publication of accurate transport properties such as thermal conductivity and viscosity of R1123, revaluation is required.

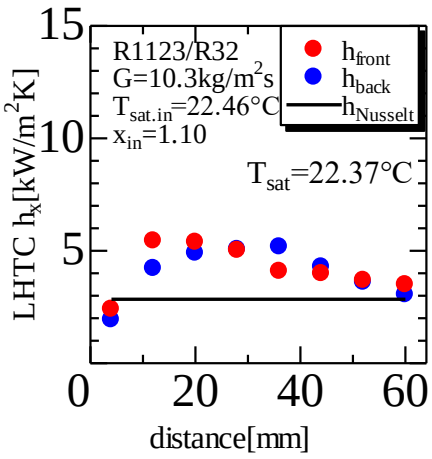

Figure 3: Local heat transfer coefficient of condensation (mixture, *x*=0.93, G = 10 kg/m^{2}s)

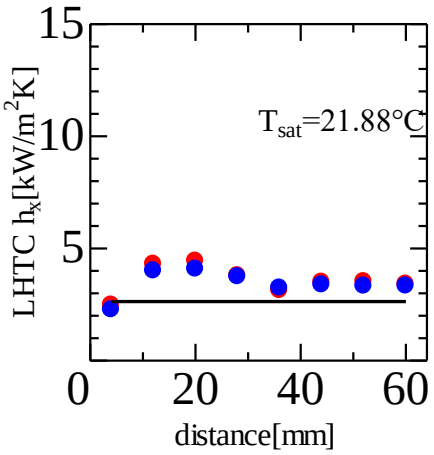

Figure 4: Local heat transfer coefficient of condensation (mixture, *x*=0.57, G = 10 kg/m^{2}s)

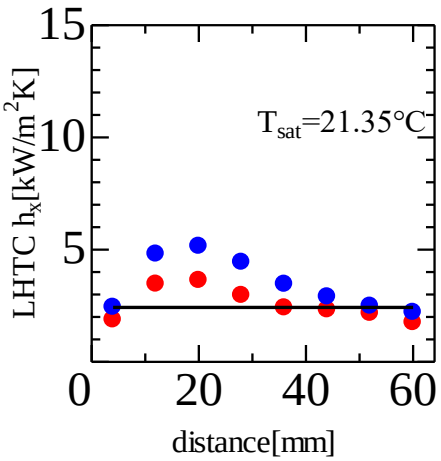

Figure 5: Local heat transfer coefficient of condensation (mixture, *x*=0.17, G = 10 kg/m^{2}s)

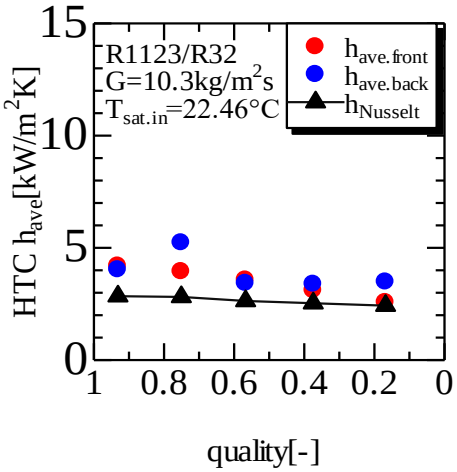

Figure 6: Average heat transfer coefficient of cross section (mixture, G = 10 kg/m^{2}s)

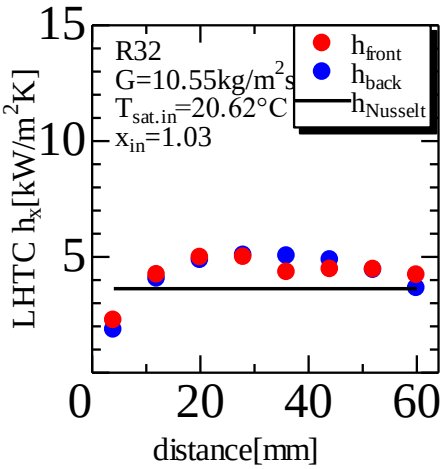

Figure 7: Local heat transfer coefficient of condensation (pure R32, *x*=0.92, G = 10 kg/m^{2}s)

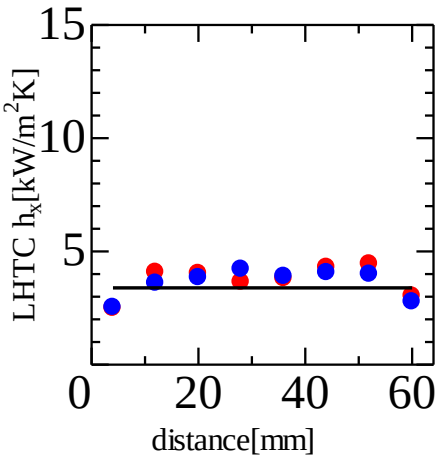

Figure 8: Local heat transfer coefficient of condensation (pure R32, *x*=0.57, G = 10 kg/m^{2}s)

3.3 Result of Evaporation

Figures 9, 10 and 11 show local heat transfer coefficient distribution in the case of the binary mixture of the evaporation experiment at x = 0.11, 0.62 and 0.99 with mass flux G = 10 [kg/m^{2}s], respectively.

As shown in figures 9 and 10, the position indicating maximum value of heat transfer coefficient is about 20 mm due to the inlet refrigerant effect and heat transfer coefficient represent the minimum value at the end face of the channel as similar to condensation experiment. In high quality condition shown in figure 11, the values of heat transfer coefficient indicate very low due to dryout of whole cross section of the channel.

Figure 12 shows the local heat transfer coefficient versus quality at the same condition in figure 9 to 11. The values of quality are average values of horizontal cross section. It is found that heat transfer coefficient slightly decreases with increasing quality.

Figures 13 and 14 show local heat transfer coefficient distribution in the case of the pure R32 of the evaporation experiment at x = 0.14 and 0.50 with mass flux G = 10 [kg/m^{2}s], respectively. Compared value of heat transfer coefficient in figure 13 with that in figure 9, value of heat transfer coefficient of pure R32 are higher than that of the binary mixture. At the middle quality condition, results shown in figure 10 and 14 can be seen same tendency. Generally, evaporation heat transfer governed by forced convection evaporation from middle to high quality region is effected by liquid thermal conductivity of the liquid phase. In this case, liquid thermal conductivity of the binary mixture is lower than pure R32 therefore the heat transfer coefficient of the binary mixture seemed to be lower.

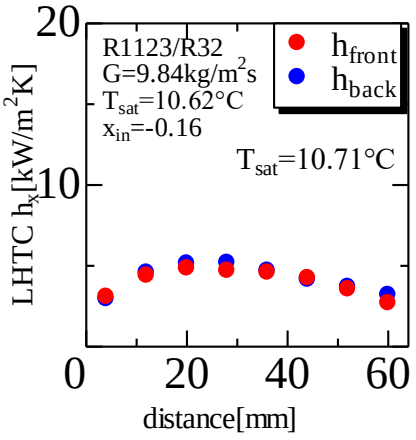

Figure 9: Local heat transfer coefficient of evaporation (mixture, x=0.11, G = 10 kg/m^{2}s)

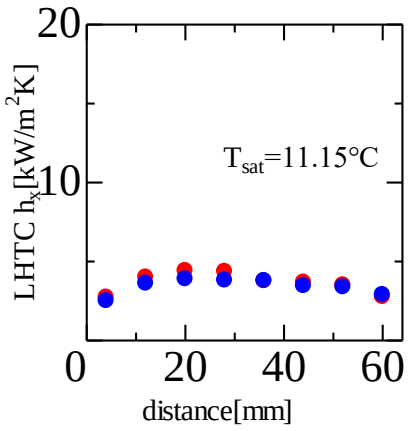

Figure 10: Local heat transfer coefficient of evaporation (mixture, x=0.62, G = 10 kg/m^{2}s)

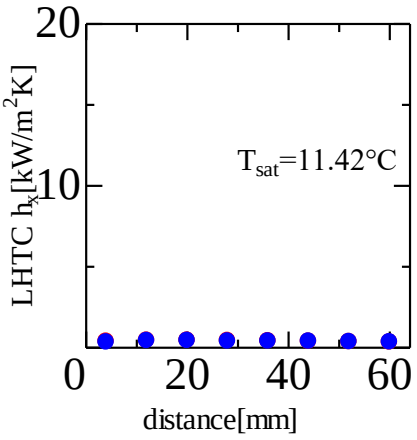

Figure 11: Local heat transfer coefficient of evaporation (mixture, x=0.99, G = 10 kg/m^{2}s)

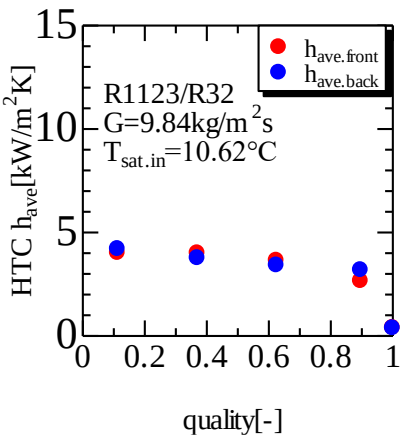

Figure 12: Average heat transfer coefficient of cross section (mixture, G = 10 kg/m^{2}s)

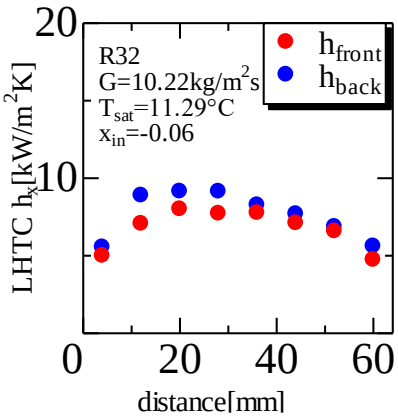

Figure 13: Local heat transfer coefficient of evaporation (pure R32, x=0.14, G = 10 kg/m^{2}s)

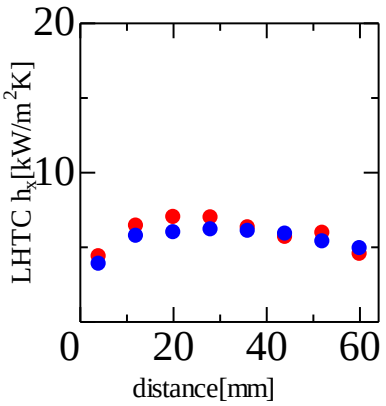

Figure 14: Local heat transfer coefficient of evaporation (pure R32, x=0.50, G = 10 kg/m^{2}s)

4. CONCLUSION

In order to obtain local heat transfer coefficient during condensation and evaporation in plate heat exchanger, a special test section has been produced where the channel is formed with two stainless steel plate having chevron grooves. Experiments on condensation and evaporation of R1123/R32 40/60 mass% binary mixture and pure R32 have been carried out and the following results were obtained.

(1) From the measured wall temperatures at 160 points in the heat transfer wall, local heat transfer behaviour is considered for condensation and evaporation experiments.

(2) In condensation experiment, local heat transfer coefficient indicates maximum value near refrigerants inlet position and minimum value at end face position of cross section of the channel.

(3) Values of condensation heat transfer coefficient of R1123/R32 binary mixture are similar to that of pure R32.

(4) In evaporation experiment, local heat transfer coefficient indicates maximum value near refrigerants inlet position and minimum value at end face position of cross section of the channel.

(5) Values of evaporation heat transfer coefficient of R1123/R32 binary mixture are lower than that of pure R32.

REFERENCES

Asano, H., Takenaka, N, Wakabayashi, T. and Fujii T., 2007, Visualization and void fraction distribution of downward gas–liquid two-phase flow in a plate heat exchanger by neutron radiography, Nuclear Instruments and Methods in Physics Research Section A: Accelerators, Spectrometers, Detectors and Associated Equipment, 542(1-3): 154-160.

Arima, H., Mishima, F., Koyama, K., Fukunami, K. and Ikegami Y., 2012, Study on void fraction measurement of ammonia boiling heat transfer in plate evaporator, Proc. 49th NHTS, NHTS: A232, (in Japanese).

Kawazoe, A., Kariya K. and Miyara A., 2015, Measurements of local heat transfer coefficient during condensation and evaporation in a plate heat exchanger, Proc. the 24th IIR International Congress of Refrigeration (ICR2015): 847 (CDROM).

Longo, G.A., 2010, Heat transfer and pressure drop during HFC refrigerant saturated vapour condensation inside a brazed plate heat exchanger, Int. J. Heat and Mass Transfer, 53: 1079-1087.

Longo, G.A., Zilio, C., Righetti, G. and Brown, J.S., 2014. Condensation of the low GWP refrigerant HFO1234ze(E) inside a brazed plate heat exchanger, Int. J. Refrigeration 38: 250-259.

Longo. G.A., 2012, Vaporisation of the low GWP refrigerant HFO1234yf inside a brazed plate heat exchanger. Int. J. Refrigeration 35: 952-961.

Longo. G.A., 2012. Condensaion of the low GWP refrigerant HFO1234yf inside a brazed plate heat exchanger. Int. J. Refrigeration 36: 612-621

Eshima, Y., Mustaghfirin, M A. and Miyara, A., 2013, An experimental study of two-phase flow in plate heat exchangers, Proc. 2013 JSRAE Annual Conf., JSRAE: 331-334 (in Japanese).

Yan, Y-Y., Lio, H.C. and Lin, T.F., 1999, Condensation heat transfer and pressure drop of refrigerant R-134a in a plate heat exchanger, Int. J. Heat and Mass Transfer, 42: 993-1006.

Miyara, A., Onaka, Y. and Koyama, S., 2012, Ways of next generation refrigerants and heat pump/refrigeration systems, Int. J. Air-Conditioning and Refrigeration, 20(1): 1130002.

Kariya, K., Mahmud, M. S., Kawazoe A. and Miyara A., Local heat transfer characteristics of the R1234ze(E) two phase flow inside a plate heat exchanger, Int. Ref. and Air Conditioning Conference (2016 Purdue conference), 2600.

Zhang, J., Desideri, A., Kærna, M., R., Ommen, T., S., Wronski, J., Haglind, F., Flow boiling heat transfer and pressure drop characteristics of R134a, R1234yf and R1234ze in a plate heat exchanger for organic Rankine cycle units, Int. J. Heat and Mass Transfer, 108: 1787-1801.

Higashi, Y. and Akasaka, R., Measurement of Thermodynamic properties for R1123 and R1123+R32 Mixture, Int. Ref. and Air Conditioning Conference (2016 Purdue conference), 2283.

ACKNOWLEDGEMENT

This study was sponsored by New Energy and Industrial Technology Development Organization (NEDO), Japan.